



Thermal Shields for Heat Loss Reduction in Siemens-Type CVD Reactors

A. Ramos,^z J. Valdehita, J. C. Zamorano, and C. del Cañizo

Instituto de Energía Solar - Universidad Politécnica de Madrid, ETSI Telecomunicación, 28040 Madrid, Spain

The use of thermal shields to reduce radiation heat loss in Siemens-type CVD reactors is analyzed, both theoretically and experimentally. The potential savings from the use of the thermal shields is first explored using a radiation heat model that takes emissivity variations with wavelength into account, which is important for materials that do not behave as gray bodies. The theoretical calculations confirm that materials with lower surface emissivity lead to higher radiation savings. Assuming that radiation heat loss is responsible for around 50% of the total power consumption, a reduction of 32.9% and 15.5% is obtained if thermal shields with constant emissivities of 0.3 and 0.7 are considered, respectively. Experiments considering different thermal shields are conducted in a laboratory CVD reactor, confirming that the real materials do not behave as gray bodies, and proving that significant energy savings in the polysilicon deposition process are obtained. Using silicon as a thermal shield leads to energy savings of between 26.5–28.5%. For wavelength-dependent emissivities, the model shows that there are significant differences in radiation heat loss, of around 25%, when compared to that of constant emissivity. The results of the model highlight the importance of having reliable data on the emissivities within the relevant range of wavelengths, and at deposition temperatures, which remains a pending issue. © 2016 The Electrochemical Society. [DOI: 10.1149/2.0171603jss] All rights reserved.

Manuscript submitted November 18, 2015; revised manuscript received December 18, 2015. Published 00 0, 2016.

Scope

90% of the polysilicon currently produced worldwide is demanded by the photovoltaic (PV) market, leaving the remaining amount for the microelectronics industry.^{1,2} The chemical route -via chemical vapor deposition (CVD) of high purity trichlorosilane (TCS) on a hot filament, the so-called Siemens technology- currently dominates polysilicon production. High quality polysilicon is obtained, at the expense of high energy consumption.^{3,4}

In the case of polysilicon for PV (also known as solar grade silicon) the process accounts for between a quarter and a third of the total energy consumption.⁵⁻⁷ Thus, lowering the energy consumption of the Siemens process is essential to achieving the two wider objectives for silicon-based PV technology: low production cost and low energy payback time.

Furthermore, current price levels also press polysilicon producers to reduce their production costs even more if they are seeking a sustainable business.⁸

As radiation heat loss is the major contributor to energy consumption,⁹ in this work the potential of thermal shields to reduce radiation heat loss in an industrial Siemens reactor is studied. Thermal (radiation) shields have been implemented in a number of CVD reactors; e.g. for layer deposition in superconducting devices or for the epitaxial growth of silicon layers.^{10,11} Several proposals have recently been made for polysilicon production,¹²⁻¹⁴ but to our knowledge quantitative analysis supported by experimental data has not been provided in any of them.

Radiation heat loss as regards thermal shields in a Siemens-type CVD reactor is studied first here using a theoretical model. Then, the theoretical results are compared with the experimental results in a laboratory Siemens reactor. Discussion of the latter will offer insights into the accuracy of theoretical calculations depending on the thermal shield materials' optical properties, highlighting the relevance of the variation in optical properties with the wavelength for thermal shield materials.

Potential to Reduce Radiation Heat Losses

First, the radiative heat transfer phenomenon is briefly described and the radiation heat loss model is presented. Then, theoretical radiation heat loss calculations for different thermal shields in an industrial Siemens reactor are put forward.

Radiative heat transfer.—Radiative heat transfer - also known as thermal radiation - describes the science of heat transfer caused by

electromagnetic waves. These electromagnetic waves have the property of traveling through a vacuum or matter-containing media. The temperature of the radiant body governs the thermal radiation emission, and it occurs in the 0.1 to 100 μm wavelength range.^{15,16} It is not the aim of this section to explain the thermal radiation phenomenon in detail, but to describe a number of concepts and properties of the radiation heat transfer mechanism that will support the arguments we develop in this document.

As regards the radiation properties, four dimensionless magnitudes are defined: absorptance (α), reflectance (ρ), transmittance (τ) and emissivity (ϵ). Absorptance, reflectance and transmittance are defined as the ratio of the total amount of radiation absorbed, reflected or transmitted by a surface to the total amount of radiation incident on the surface, respectively. The emissivity⁴ Emissivity is defined as the ratio of the power per unit area radiated by a surface to the power per unit area radiated by a black body at the same temperature. These properties for real surfaces are dependent on temperature, direction and wavelength. The relationship indicated in Equation 1 is obtained by applying the energy balance to any real surface.

$$\alpha + \rho + \tau = 1 \quad [1]$$

In addition, according to Kirchhoff's law, all opaque surfaces ($\tau = 0$) reach $\epsilon_\lambda(\lambda, T) = \alpha_\lambda(\lambda, T)$.^{15,16}

A black body is defined as any body that emits and absorbs the maximum possible radiation in all wavelengths, that is: $\alpha = 1$, $\rho = \tau = 0$. Plack's law defines the spectral radiated power of a black body. In addition, according to Stefan-Boltzmann's law the expression for the total radiation emitted per unit area of a black body is indicated in Equation 2; where T is the temperature and σ the Boltzmann constant.

$$E_b(T) = \sigma T^4 \quad [2]$$

However, the majority of the surfaces do not behave as black bodies; thus, the gray body concept arises. A gray body is any opaque body ($\tau = 0$, $\alpha + \rho = 1$) whose reflectance, absorptance and emissivity properties are non dependent on the wavelength. The behavior of many real surfaces can be approximated to that of a gray body; in Equation 3 the expression of the total radiation emitted per unit area of a gray body is presented.

$$E_g(T) = \epsilon_g \sigma T^4 \quad [3]$$

The parameter ϵ_g corresponds to the emissivity of a gray body. But, being more rigorous, real surfaces do not necessary behave as gray bodies, and their properties vary with the wavelength for a

^zE-mail: alba.ramos@ies-def.upm.es

⁴Some authors refer to this parameter as 'emittance'. In this work emissivity and emittance are the same concept; however, there is a subtle difference between the two.¹⁶

98 given temperature. These surfaces radiate a different fraction ε_λ at
99 each wavelength; thus, the expression of the total radiation emitted
100 per unit area of a real surface is indicated in Equation 4. Note that the
101 parameter ε_r in Equation 4 is calculated by means of Equation 5; that
102 is, integrating ε_λ along all the radiation spectrum.

$$E_{real}(T) \cong \varepsilon_r \sigma T^4 \quad [4]$$

$$\varepsilon_r = \frac{\int_0^\infty \varepsilon_\lambda E_{b\lambda} d\lambda}{\int_0^\infty E_{b\lambda} d\lambda} \quad [5]$$

104 **Real material properties.**—As said previously, the radiative prop-
105 erties of real materials are not necessarily those of gray bodies. The
106 difficulty is how to characterize the radiative properties of a selected
107 material under working conditions. The reflectance (ρ_λ) and transmit-
108 tance (τ_λ) of real surfaces can be determined by means of the Fourier
109 transform infrared spectroscopy (FTIR);¹⁷ thus, from Equation 1 absorp-
110 tivity (α_λ) can be obtained. But these measurements are typically
111 performed at room temperature; there are no overall techniques for
112 the measurement of radiative properties at high temperatures. It is true
113 that for certain materials, in particular for some metals, it is accept-
114 able to consider that their radiative properties remain constant with
115 temperature, although this cannot be easily generalized.^{16,18,19}

116 **Radiation heat loss model.**—A radiation heat loss model for heat
117 loss calculations in a Siemens-type reactor was presented and de-
118 scribed in detail in Ref. 20, and validated in Ref. 21. It is further
119 developed within the framework of this research to broaden its appli-
120 cability and account for materials that do not behave as gray bodies.

121 One parameter needs to be defined for radiation heat loss calcu-
122 lations: radiosity (J), the rate of outgoing radiant heat per unit area
123 from a surface. It is the sum of the directly emitted heat flux (E) and
124 the reflected incoming radiant heat flux from the surface (G). The
125 fraction of heat flux from one surface to another is determined by the
126 so-called configuration factor, or geometrical factor. The calculation
127 of the configuration factors (F_{i-j}) is made using a geometric Hottel's
128 crossed-string method.²² In the present case note that the rods and the
129 reactor wall have a cylindrical geometry.

130 If the material properties, the geometrical arrangement, the surface
131 temperatures and the incoming and directly emitted radiant heat flux
132 are known, the net heat flux exchanged (Q) in Watts from any surface
133 (S_i), is obtained from the difference between the radiosity and the
134 incoming radiant heat flux. Then, the net radiation heat flux exchanged
135 for a certain surface i can be expressed as shown in Equation 6.

$$Q_i = S_i \cdot (J_i - G_i) = S_i \cdot J_i - \sum_{j=1}^n S_j \cdot F_{j-i} \cdot J_j \quad [6]$$

136 For a Siemens reactor of $n-1$ rods, a n -equations system needs to
137 be solved, as the reactor wall is considered as an additional surface.
138 The radiosities of each surface (J_i) are the unknowns of the system.
139 The temperature of the rod surfaces and the reactor wall is known, as
140 is the corresponding surface emissivities. Once the J_i is obtained for
141 the n surfaces, the incoming radiant heat flux per unit area (G_i) is also
142 known. Thus, the net radiation heat exchanged by each surface (Q_i)
143 is obtained by substituting J_i and G_i in Equation 6.

144 To account for emissivity variations with the wavelength, radiation
145 heat loss is obtained by means of Equations 7, 8, 9 and 10, which are
146 solved independently for each wavelength

$$S_i \cdot \frac{1}{1 - \varepsilon_i(\lambda)} \cdot J_i(\lambda) - \sum_{j=1}^n S_j \cdot F_{i-j} \cdot J_j(\lambda) = S_i \cdot \frac{\varepsilon_i(\lambda)}{1 - \varepsilon_i(\lambda)} \cdot \sigma \cdot T_i^4 \quad [7]$$

$$E_i(\lambda) = \varepsilon_i(\lambda) \cdot \sigma \cdot T_i^4 \quad [8]$$

$$G_i(\lambda) = \frac{1}{1 - \varepsilon_i(\lambda)} \cdot (J_i(\lambda) - E_i(\lambda)) \quad [9]$$

$$Q_i(\lambda) = S_i \cdot (J_i(\lambda) - G_i(\lambda)) \quad [10]$$

where $i = 1, \dots, n$.

The net heat flux exchanged (Q_i) in Watts by any surface (S_i),
is obtained by integrating $Q_i(\lambda)$ along all the radiation spectrum. In
Equation 11 the net heat flux exchanged by a surface is presented;
 $E_b(\lambda)$ is the total radiation emitted per unit area of a black body
indicated in Equation 2.

$$Q_i = \frac{\int_0^\infty Q_i(\lambda) E_b(\lambda) d\lambda}{\int_0^\infty E_b(\lambda) d\lambda} \quad [11]$$

This radiative model allows extra surfaces in the Siemens reactor
to be considered and their positive or negative effect on heat savings
studied. This can be the case of a thermal shield. A thermal shield
is a cylinder surrounding the polysilicon rods and placed between
them and the reactor wall. The presence of this shield may block
a significant part of the radiated heat that otherwise would be lost
through the reactor wall.

Now, the net heat flux exchanged (Q_i) in Watts by any surface
(S_i), is again obtained by integrating $Q_i(\lambda)$ along all the radiation
spectrum; but by replacing Equation 7 with Equations 12–15 (where
 $i = 1, \dots, m-1$, and m is the number of thermal shields considered).

$$S_i \cdot \frac{1}{1 - \varepsilon_i(\lambda)} \cdot J_i(\lambda) - \sum_{j=1}^m S_j \cdot F_{i-j} \cdot J_j(\lambda) = S_i \cdot \frac{\varepsilon_i(\lambda)}{1 - \varepsilon_i(\lambda)} \cdot \sigma \cdot T_i^4 \quad [12]$$

$$S_m \cdot \frac{1}{1 - \varepsilon_m(\lambda)} \cdot J_m(\lambda) - \sum_{j=1}^m S_m \cdot F_{m-j} \cdot J_j(\lambda) = S_m \cdot \frac{\varepsilon_m(\lambda)}{1 - \varepsilon_m(\lambda)} \cdot \sigma \cdot T_m^4 \quad [13]$$

$$\left(S_m \cdot \frac{\varepsilon_s(\lambda)}{1 - \varepsilon_s(\lambda)} + \frac{1}{\gamma(\lambda)} \right) \cdot \sigma T_m^4 - S_m \cdot \frac{\varepsilon_s(\lambda)}{1 - \varepsilon_s(\lambda)} \cdot J_m(\lambda) = \frac{\sigma T_n^4}{\gamma(\lambda)} \quad [14]$$

$$\gamma(\lambda) = \frac{1}{S_m \cdot \varepsilon_s(\lambda)} + \frac{1}{S_n} \cdot \left(\frac{1}{\varepsilon_n(\lambda)} - 1 \right) + \left(\frac{2}{\varepsilon_s(\lambda)} - 1 \right) \cdot \sum_{i=m+1}^{n-1} \frac{1}{S_i} \quad [15]$$

Note that even if the emissivity values now considered may be
wavelength dependent, materials still are considered opaque ($\tau = 0$).

Theoretical calculations.—The potential of different thermal
shields for radiation heat savings in an industrial Siemens reactor is
studied here. The equations presented above are applied to a 36-rod,
state-of-the-art Siemens reactor, and as a first approach, the emissivity
of the materials is considered constant and wavelength independent.
The initial and final diameter of the polysilicon rods is 0.7 and 13 cm,
respectively, and their length is 2 m.

In Figure 1 the heat loss due to radiation in Watts (W) throughout
a polysilicon deposition process for a constant surface temperature of
1150°C is shown; the curves correspond to the case with no thermal
shield and four cases with thermal shields. The emissivities of the
thermal shields are 0.3, 0.45, 0.55 and 0.7. In Table I the theoretical
radiation heat loss savings for the aforementioned thermal shields are
presented. The radiation heat loss savings, compared to the heat loss
if no thermal shield is considered, are 65.8, 52.6, 44.3 and 30.5% for
thermal shield emissivities (ε) of 0.3, 0.45, 0.55 and 0.7, respectively.
This means, assuming that the radiation heat loss is responsible for
around 50% of the total power consumption, that with a thermal shield
with $\varepsilon = 0.3$ a reduction in power consumption of 32.9% is obtained,
while for $\varepsilon = 0.7$ the reduction would be of 15.5%.

The temperature reached by the different thermal shields depend-
ing on their emissivity is presented in Figure 2. In all cases, and from
the beginning of the process, these temperatures are above 850°C,
which will result in polysilicon deposition on these surfaces. Thus,

Table I. Theoretical radiation heat loss savings for different thermal shields.

Thermal shield ϵ [-]	Radiation heat loss savings [%]
0.3	65.8
0.45	52.6
0.55	44.3
0.7	30.5

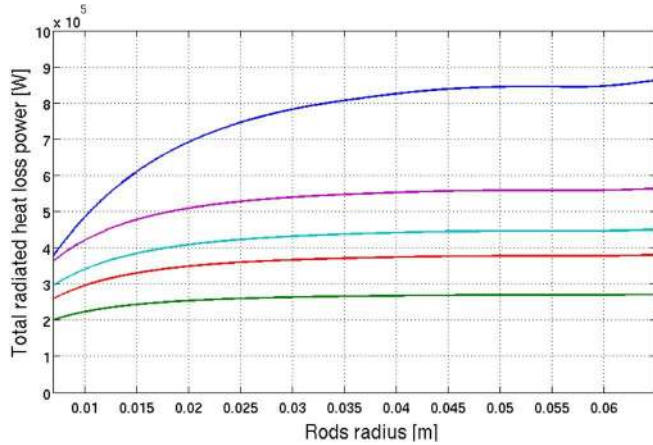


Figure 1. Radiation heat loss for a 36-rod Siemens reactor considering different thermal shields. No thermal shield (blue), $\epsilon = 0.7$ (purple), $\epsilon = 0.55$ (cyan), $\epsilon = 0.45$ (red), $\epsilon = 0.3$ (green).

197 after a few minutes into the deposition process the thermal shield's
198 surface emissivity will be 0.7, that of silicon at high temperatures.²³
199 Furthermore, contamination issues can arise unless the shields are of
200 a highly pure material. One way to overcome these drawbacks would
201 be to use a thermal shield made of purified silicon.¹² Not only will it
202 avoid contamination, but one can also collect the silicon deposited on
203 the shields, adding it to the silicon produced in a batch.

204 The potential of thermal shields can be compared to the use of a
205 polished or a reflective-coated inner wall of a reactor, which will lower
206 the wall emissivity. For a given growth rate, and knowing the power
207 consumption throughout a deposition process, and the initial and the
208 final diameters of the polysilicon rods, the energy consumption in
209 kWh/kg can be calculated. In Figure 3 the kWh/kg ratio for the case
210 of a reflective-coated wall is compared to those considering a silicon
211 thermal shield, no thermal shield and a thermal shield of $\epsilon = 0.3$. For
212 the calculations in Figure 3 the emissivity of the wall and the thermal

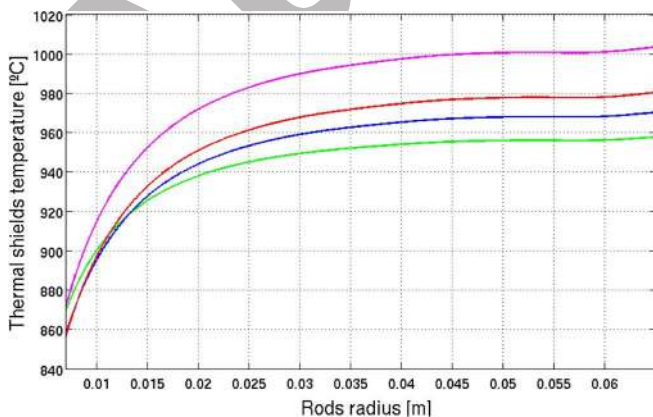


Figure 2. The temperature of thermal shields depending on their emissivity (ϵ) throughout a deposition process. Thermal shield emissivities: $\epsilon = 0.7$ (purple), $\epsilon = 0.55$ (red), $\epsilon = 0.45$ (blue), $\epsilon = 0.3$ (green).

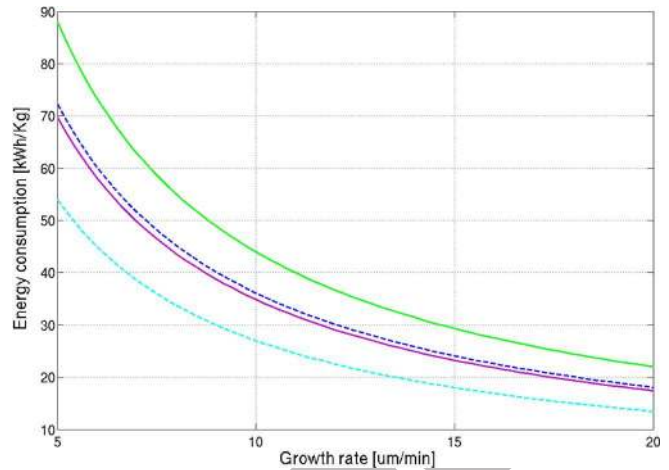


Figure 3. Total power consumption of a 36-rod Siemens reactor for different growth rates considering: no thermal shield $-\epsilon_{wall} = 0.5$ - (green), silicon thermal shield $-\epsilon = 0.7$ - (purple), thermal shield with $\epsilon = 0.3$ (cyan) and no thermal shield and polished reactor wall $-\epsilon_{wall} = 0.3$ - (blue).

shields is considered constant throughout a deposition process; and the
radiation heat loss is 50% of the total power consumption. The lowest
kWh/kg ratio is obtained for a low emissivity thermal shield, and the
kWh/kg ratio for that with a silicon thermal shield and a polished
inner wall are quite close. However, note that the low emissivity
thermal shield and the polished walls will not maintain their initial
emissivities for more than a short period of time, as silicon or a silane-
based compound will deposit. After a few minutes into the deposition
process the blue curve will start to move slowly upwards until it
reaches the green curve; and the cyan curve will quickly move to
behave like the purple curve. Thus, the effect of a thermal shield is
more efficient in terms of energy savings than considering a polished
reactor wall; this statement is true even when considering a high initial
emissivity value for the thermal shield (e.g., $\epsilon = 0.7$).

Laboratory Scale Experiments

A number of experiments considering thermal shields are conducted in a laboratory Siemens reactor,²⁴ and the effect on radiation heat savings obtained is put forward.

Since the temperature of the thermal shield in the laboratory reactor will be lower than in the industrial case, the laboratory prototype allows us to test the effect of thermal shields with different emissivities. The key parameter for the selection of the thermal shield material is the emissivity (ϵ); but also, the material selected must be easily machinable, and available with the geometries and thickness required for its assembly inside the reactor chamber, so its mechanical strength must be assured. The following materials are evaluated: molybdenum, boron nitride, stainless steel, aluminum oxide (alumina), zirconium, graphite foil and silicon. Some of the relevant properties of these materials are presented in Table II; the values shown are considered wavelength independent since this dependence is unknown.

Table II. Properties of different materials considered for the thermal shields.^{25,26}

Material	ϵ [-] ($T = 25^\circ\text{C}$)	ϵ [-] ($T \sim 600^\circ\text{C}$)	Ease of machining
Molybdenum	-	0.8-0.9	Medium
Stainless steel	0.6-0.8	0.7-0.9	Low
Alumina	-	0.3-0.4	Medium
Boron nitride	0.9-0.95	-	Medium
Zirconium	-	0.1-0.3	High
Graphite foil	0.7-0.9	0.4-0.6	Low
Silicon	-	0.7	Medium

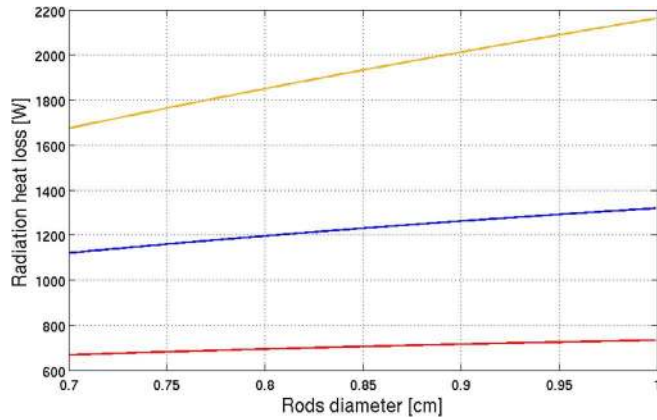


Figure 4. Radiation heat loss in the laboratory Siemens reactor for a 7-rod configuration considering a silicon thermal shield (blue), a low emissivity thermal shield $\epsilon = 0.3$ - (red) and without thermal shield (orange).

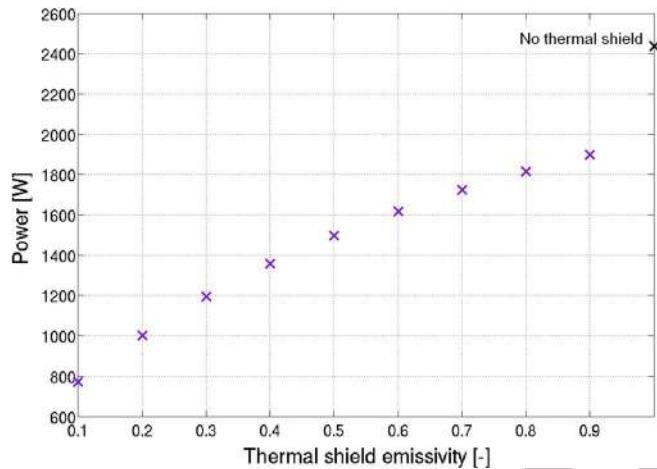


Figure 5. Laboratory Siemens reactor power consumption (P) predicted in theory for different thermal shield emissivities and for the case of no thermal shield considering a 7-rod configuration.

243 First, the radiation heat loss equations with thermal shields are
 244 applied to the laboratory Siemens reactor. The radiation heat loss
 245 for a 7-rod configuration with a low emissivity shield, with a silicon
 246 thermal shield and without thermal shield is presented in Figure 4; it
 247 can be seen how the lowest radiation heat losses are obtained for a low
 248 emissivity thermal shield. The temperatures reached by the thermal
 249 shields are in the range of 600-750°C.

250 The power consumption predicted by the model for different thermal
 251 shield emissivities and for that of no thermal shield, are presented
 252 in Figure 5. For these calculations a constant deposition temperature
 253 of 1100°C, the same growth rate and the same duration of the depo-
 254 sition processes, is considered, thus averaging the measured data. It
 255 can be seen that the lower emissivity of the thermal shield, the higher
 256 radiation heat savings.

257 **Experiments with thermal shields.**—A 7-rod configuration is cho-
 258 sen as a compromise solution between a dense compactness - a large
 259 number of rods - and the size of the reactor chamber. The length of
 260 the rods is 10 cm and their initial diameter is around 0.7 cm.

261 From the thermal shield materials listed in Table II, the following
 262 have been selected for testing: silicon, alumina and stainless steel.
 263 Different thickness of the selected materials are considered, and in
 264 some cases the outer surface of the thermal shields is silver coated^b.

^bThe silver coatings deposited are a few hundred nanometers thick.

Table III. Experiments conducted with 7-rod configuration in the laboratory Siemens reactor.

Experiment name	Description
No shield (No)	Without any thermal shield
Silicon shield (Si1)	Multi-crystalline silicon thermal shield (290 $\mu\text{m}/\text{layer}$; 3 layers)
Silicon shield (Si2)	Mono + Multi-crystalline silicon thermal shield (400 + 290 μm : 1 + 1 layers)
Silicon shield (Si3)	Mono + Multi-crystalline silicon thermal shield (400 + 290 \times 4 μm ; 1 + 4 layers)
Alumina shield (Alu1)	Alumina shield (1 mm thick)
Alumina shield (Alu2)	Alumina shield silver coated (1 mm thick)
Steel shield (Ste)	Stainless steel shield (1 mm thick)

Table IV. Experimental data obtained for the 7-rod configuration experiments: 'silicon shields'.

Experiment	(No)	(Si1)	(Si2)	(Si3)
$T_{\text{deposition}}$ [°C]	1106	1101	1108	1108
Si deposited [gr]	50.7	61.9	59.3	59.8
$\text{Power}_{\text{average}}$	2343	1979	2042	2122
Time [min]	392	406	385	375
T_{wall} [°C]	280	233	184	181
T_{shield} [°C]	-	678	641	616
Growth rate [$\mu\text{m}/\text{min}$]	2.9	3.5	3.6	3.6
Consumption [kWh/kg]	311	216	221	222
Energy savings [%]	-	28.4	26.8	26.5

265 The emissivity of silver is very low ($\epsilon \sim 0.02$ - 0.05), so if this coating
 266 withstands the process temperatures, it will act as a mirror making a
 267 non-opaque body behave almost as if it were.

268 The relevant data related to these experiments is presented in the
 269 following tables. First, the different thermal shields are described and
 270 related to their corresponding label in Table III. Then, the experimental
 271 results are grouped together in 'silicon shields' and 'alumina and
 272 stainless steel shields'; Tables IV and V, respectively.

273 From the data presented in Table IV, the energy savings obtained
 274 with the different silicon thermal shields are similar. The reduction
 275 in the kWh/kg ratio obtained considering thermal shields related to
 276 experiment (No) are between 26.5 and 28.4%. All these experiments
 277 were conducted under similar conditions and their duration is similar.
 278 Despite the fact that the deposition surface temperature is in all cases
 279 around 1100°C, there is a difference in the growth rate obtained in
 280 experiment (No). This is so because the presence of a thermal shield
 281 changes the distribution of the gas temperature, and higher tempera-
 282 tures are achieved in the gas surrounding the silicon rods.

283 From the data presented in Table V, the energy savings in kWh/kg,
 284 compared with experiment (No), vary between 15.1 and 30.7%. The

Table V. Experimental data obtained for the 7-rod configuration experiments: 'alumina and stainless steel shields'.

Experiment	(No)	(Alu1)	(Alu2)	(Ste)
$T_{\text{deposition}}$ [°C]	1106	1107	1108	1098
Si deposited [gr]	50.7	65.3	53.7	49.3
$\text{Power}_{\text{average}}$	2343	2333	1669	1915
Time [min]	392	430	404	388
T_{wall} [°C]	280	142	175	152
T_{shield} [°C]	-	736	705	570
Growth rate [$\mu\text{m}/\text{min}$]	2.9	3.6	3.2	3.0
Consumption [kWh/kg]	311	256	205	251
Energy savings [%]	-	15.1	30.7	16.8

285 kWh/kg values in the laboratory scale reactor are several times higher
 286 than those found in industrial processes, mainly since the process pres-
 287 sure is 6-7 times lower. Comparing experiments (Alu1) and (Alu2),
 288 the silver coating seems to be effective; however its behavior differs
 289 from that expected from its theoretical ϵ (further explanations will be
 290 presented in Discussion on energy savings section).

291 Lastly, in experiments conducted with silicon thermal shields etch-
 292 ing is detected on the surface of the shields. This is attributed to the
 293 presence of SiCl_4 as a by-product of the reduction reaction. The oc-
 294 currence of this phenomenon versus polysilicon deposition depends
 295 on the mol fraction of SiCl_4 , which will depend on the deposition sur-
 296 face temperature.^{27,28} High SiCl_4 concentrations and low temperatures
 297 favor the etching. However, as already explained, under industrial de-
 298 position conditions the temperature of the thermal shields will be
 299 such that polysilicon will be deposited on the thermal shields, and no
 300 etching is expected.

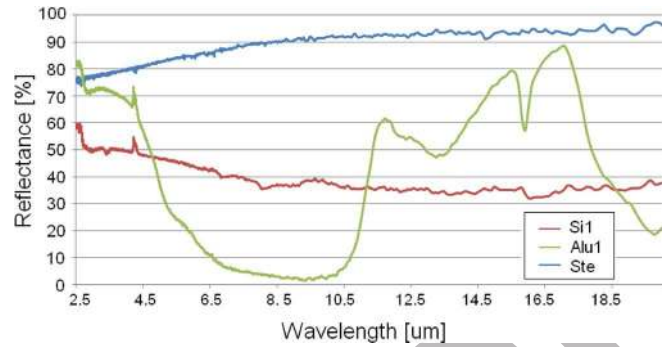
301 **Discussion on energy savings.**—From the above, energy savings
 302 have been confirmed for the 7-rod configuration experiments consid-
 303 ering different thermal shields.

304 If the experimental data from Tables IV and V (average power
 305 consumption and energy savings) is compared with the theoretical cal-
 306 culations for different thermal shields (Figure 5), a good agreement
 307 for the case of no thermal shields is obtained; differences between
 308 both values are under 3.8%. Note that our calculations consider con-
 309 stant deposition conditions, while the experimental conditions of the
 310 deposition process vary slightly from one experiment to another.

311 For the experiments conducted with thermal shields, the averaged
 312 power consumption and energy savings obtained vary between 1667-
 313 2333 W and 15.1–30.7%, respectively. According to data presented in
 314 Figure 5, the previous values correspond to thermal shield emissivities
 315 above 0.6. In the case of the silicon thermal shields, the energy savings
 316 obtained correspond to $\epsilon = 0.7$ –0.8, for the alumina shields to $\epsilon >$
 317 0.9, for the silver coated alumina shield to $\epsilon = 0.6$ –0.7; and for the
 318 stainless steel shield to $\epsilon > 0.9$. These ϵ values do not correspond
 319 to those found in the bibliography assuming the gray body approach,
 320 which is no surprise since the gray body approach simplifies much of
 321 the radiative behavior of real bodies.

322 **Reflectance, transmittance and emissivity measurements.**—With
 323 the aim of clarifying the real emissivity of the thermal shield materials
 324 tested in the laboratory Siemens reactor, reflectance (ρ) and transmittance
 325 (τ) measurements for different λ are taken. Both, $\rho(\lambda)$ and
 326 $\tau(\lambda)$, can be measured directionally or integrated; in the present case
 327 integrated measurements are suitable since the materials considered
 328 do not have specular surfaces. These measurements are conducted at
 329 room temperature.

330 In Figure 6 the integrated transmittance measurements, within the
 331 wavelength range $\lambda \in (2.5\text{--}20) \mu\text{m}$, for different thermal shields are
 332 presented. In all cases, noticeably for the silicon shield, the integrated
 333 transmittance is $\tau \neq 0$. Measurements for a silicon, alumina and
 334 stainless steel thermal shields are presented in Figure 6. The integrated
 335 transmittance measured is on average 41.3, 8.1 and 0.5% for the



336 **Figure 7.** Integrated reflectance (ρ) of: 290 μm multi-crystalline silicon (red),
 337 1 mm alumina (green) and 1 mm stainless steel (cyan).

338 290 μm multi-crystalline, 1 mm alumina and 1 mm stainless steel
 339 samples, respectively.

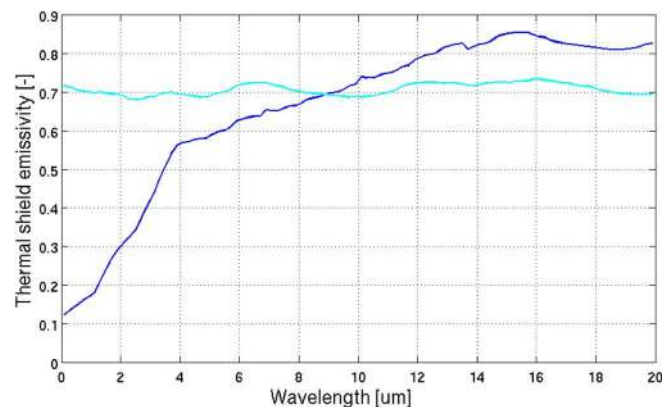
340 Integrated reflectance measurements are also conducted; $\rho(\lambda)$ for
 341 $\lambda \in (2.5\text{--}20) \mu\text{m}$ for silicon, alumina and stainless steel are presented
 342 in Figure 7. From Figure 7, the averaged reflectance of the silicon
 343 sample is 40%, while the respective values for that of alumina and the
 344 stainless steel samples are 48.1 and 92.8%, respectively.

345 From the average values of the aforementioned transmittance and
 346 reflectance integrated measurements, only the stainless steel sample
 347 presents a very low transmittance. Materials experimentally tested in
 348 the laboratory Siemens reactor at room temperature definitely do not
 349 behave as gray bodies, and similar behavior can be expected at higher
 350 temperatures.^{18,19} The latter explains the differences between the pre-
 351 dicted energy savings and the empirically obtained ones. The next
 352 section discusses the effect that the wavelength-dependent emissivities
 353 can have on the radiation heat losses.

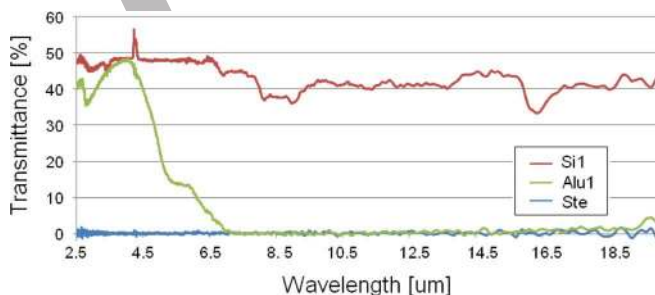
352 **Discussion on the Contribution to the Radiation Heat Loss Model**

353 The model for radiation heat loss is applied here for the radi-
 354 ation heat loss calculations of a 36-rod industrial Siemens reactor,
 355 considering thermal shields that do not behave as gray bodies. Two
 356 hypothetical thermal shields with an averaged $\epsilon(\lambda) = 0.7$ are con-
 357 sidered, with an emissivity variation presented in Figure 8. It can be
 358 seen that $\epsilon(\lambda)$ of material 1 is approximately constant, while $\epsilon(\lambda)$ of
 359 material 2 is heavily dependent on the wavelength.

360 The radiation heat loss for $\lambda \in (0.1, 20) \mu\text{m}$, calculated for a 36-rod
 361 industrial Siemens reactor, is presented in Figure 9. The two scenarios
 362 presented; hereinafter scenarios 1 and 2, correspond to material 1 and
 363 material 2 thermal shields, respectively. In both cases, the radiation



364 **Figure 8.** Emissivity $\epsilon(\lambda)$ for two different thermal shield materials: material
 365 1 (cyan) and material 2 (blue). In both cases, the averaged $\epsilon(\lambda) = 0.7$.



366 **Figure 6.** Integrated transmittance (τ) of: 290 μm multi-crystalline silicon
 367 (red), 1 mm alumina (green) and 1 mm stainless steel (cyan).

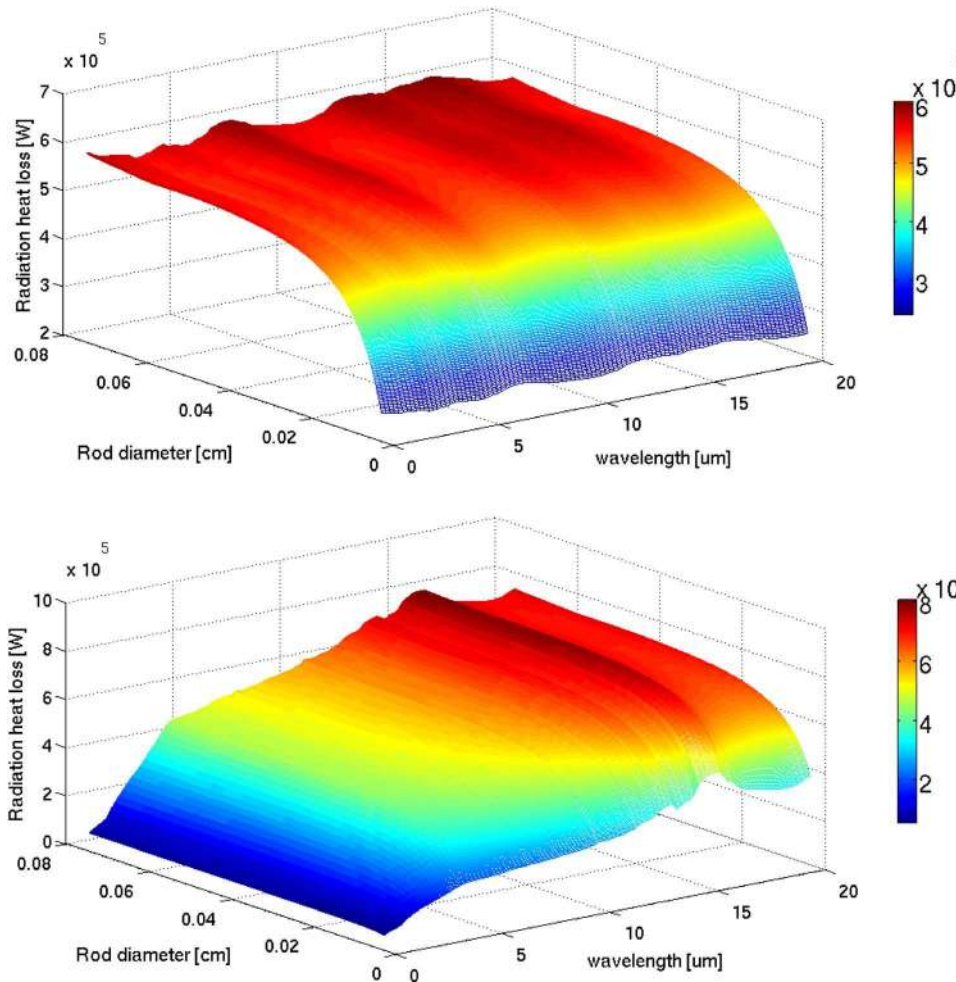


Figure 9. Radiation heat loss for different wavelengths for two different thermal shield materials: material 1 (top) and material 2 (bottom).

364 heat loss variation with λ is similar to the corresponding variation in
 365 $\epsilon(\lambda)$ of the shield material considered.

366 When the surfaces presented in Figure 9 are integrated along the
 367 entire radiation spectrum, the radiation heat loss values presented in
 368 Figure 10 for scenarios 1 and 2 are obtained. This curves are pre-

369 sented together with the corresponding curve if a constant emissivity
 370 for the thermal shield $\epsilon(\lambda) = 0.7$ is considered - scenario 3. It can
 371 be appreciated how the scenarios 1 and 3 are quite close, but great
 372 differences in radiation heat loss are obtained between scenarios 1 and
 373 3, and scenario 2; the averaged differences are above 25%. As regards
 374 the thermal shield temperature, results obtained for scenarios 1 and 3
 375 are also quite close; the temperature of the shields is around 870°C
 376 at the beginning of the deposition process, increasing rapidly until it
 377 reaches around 1000°C at the end of the process. In scenario 2, the
 378 thermal shield temperature has a similar behavior with temperature
 379 values that go from 860 to 975°C.

380 The aforementioned differences above are explained since not all
 381 wavelengths contribute to the same extent to the radiation heat loss;
 382 in particular for these three scenarios, the greatest contribution of $\epsilon(\lambda)$
 383 occurs in the range $\lambda \in (1-6) \mu\text{m}$.

384 These results highlight the importance of having reliable data on
 385 the emissivities in the relevant range of wavelengths, and for the
 386 application of silicon CVD, at deposition process temperatures, which
 387 remains pending.

Conclusion

388 A radiation model for heat loss calculations in a Siemens-type
 389 reactor has been presented, in which the fraction of energy leaving a
 390 certain surface that arrives at another surface is evaluated using the
 391 geometric Hottel crossed-string method, and the effect of the emissiv-
 392 ity variation with the wavelength is taken into account. A significant
 393

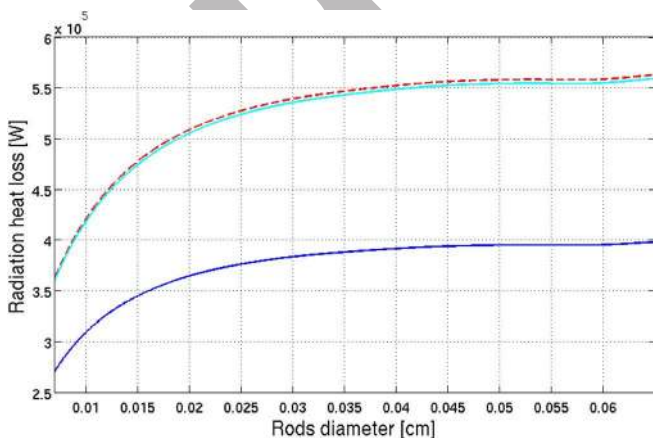


Figure 10. Radiation heat loss for different thermal shield materials: material 1 (cyan), material 2 (blue), obtained by integrating Figure 9 along all the radiation spectrum. The case of a material with a constant $\epsilon(\lambda) = 0.7$ is presented for comparison (red).

394 potential for reducing radiation heat loss in Siemens reactors has been
 395 identified, considering different thermal shields. The model shows
 396 that materials with lower surface emissivities lead to higher radiation
 397 heat loss savings. The effect of a thermal shield is also more efficient
 398 in terms of energy savings than considering a polished reactor wall,
 399 even for a thermal shield with a high initial emissivity value.

400 Experiments considering different thermal shields are conducted
 401 in a laboratory Siemens reactor. It has been experimentally shown
 402 that significant energy savings in the polysilicon deposition process
 403 are obtained.

404 Silicon thermal shields have some advantages in terms of pre-
 405 venting contamination and collecting the silicon deposited on them,
 406 and energy savings of between 26.5-28.5% have been experimentally
 407 proven.

408 Reflectance and transmittance measurements as a function of
 409 wavelength are taken for the materials tested, proving that they do
 410 not behave as gray bodies at room temperature, and similar behavior
 411 can be expected at higher temperatures. Results highlight the impor-
 412 tance of having reliable emissivity data on the materials involved at
 413 deposition temperatures, which remains pending.

414 Acknowledgments

415 The Spanish *Ministerio de Economía y Competitividad* is acknowl-
 416 edged for its support through the IPT 2012-0340-120000 project and
 417 *Comunidad de Madrid* through the MADRID-PV S2013/MAE-2780
 418 project.

419 Ángel Morales, from the Centro de Investigaciones Energéticas
 420 Medioambientales y Tecnológicas (CIEMAT), Spain is acknowledged
 421 for his contribution to the reflectance and transmittance measurements.

References

422 1. K. Hesse, E. Schindlbeck, E. Dornberger, and M. Fischer, "Status and Develop-
 423 ment of Solar-Grade Silicon Feedstock," *24th European Photovoltaic Solar Energy*
 424 *Conference*, 883 (2009).
 425 2. R. Berstein, "A shortage hits solar power," *The Wall Street Journal*, (2006).
 426 3. A. F. B. Braga, S. P. Moreira, P. R. Zampieri, J. M. G. Bacchin, and P. R. Mei, "New
 427 processes for the silicon production of solar-grade polycrystalline silicon: A review,"
 428 *Solar Energy Materials and Solar Cells*, **92**, 418 (2008).
 429 4. C. Wang, T. Wang, P. Li, and Z. Wang, "Recycling of SiCl₄ in the manufacture of
 430 granular polysilicon in a fluidized bed reactor," *Chemical Engineering Journal*, **220**,
 431 (2013).

5. B. Ceccaroli and O. Lohne, *Handbook of Photovoltaic Science and Engineering, in:*
 432 *Solar Grade Silicon Feedstock*, 2nd Edition, pp. 169-217 (2011). 433
 6. E. Alsema and M. de Wild-Scholten, "Reduction of the environmental impacts in
 434 crystalline silicon module manufacturing," *22nd European Photovoltaic Solar Energy*
 435 *Conference and Exhibition*, pp. 829-836, (2007). 436
 7. S. Singer, "Photovoltaics: Getting Cheaper," *EcoQueen of Green*, (2007). 437
 8. T. F. Ciszek, "Photovoltaic materials and crystal growth research and development in
 438 the gigawatt era," *Journal of Crystal Growth*, **393**, 2 (2014). 439
 9. A. Ramos, A. Rodríguez, C. del Cañizo, J. Valdehita, J. C. Zamorano, and A. Luque,
 440 "Heat losses in a CVD reactor for polysilicon production: Comprehensive model and
 441 experimental validation," *Journal of Crystal Growth*, **402**, 138 (2014). 442
 10. H. Griss, B. Caussat, H. Vergnes, and J. P. Couder, "An improvement in the be-
 443 havior of LPCVD reactors: the dead zones reducers," *Chemical Vapor Deposition:*
 444 *Proceedings of the Fourteenth International and EUROCVD-11*, 194-201, 1997. 445
 11. M. A. Gallivan, D. G. Goodwin, and R. M. Murray, "A Design Study for Thermal
 446 Control of a CVD Reactor for YBCO," *Proceedings of the 1998 IEEE International*
 447 *Conference on Control Applications*, Italy, 1998. 448
 12. C. del Cañizo, G. del Coso, A. Luque, and J. C. Zamorano, "Thermal shield for
 449 silicon production reactors," [Pat.: WO 2012025513 A1], (2012). 450
 13. G. Pazzaglia, M. Fumagalli, and M. Kulkarni, "Bell jar for siemens reactor including
 451 thermal radiation shield," [Pat.: WO 2011128729 A1], (2011). 452
 14. J. Lee, J. Kim, S. Lee, and L. C. Winterton, "Chemical vapor deposition reactor having
 453 a radiant heat barrier layer for improving energy efficiency," [Pat.: WO 2011068283
 454 A1], (2011). 455
 15. F. Kreith and M. Bohn, *Heat transfer by radiation, Principles of heat transfer*, 6th
 456 Ed., Thomson, pp. 539-626, (2002). 457
 16. M. F. Modest, *Radiative heat transfer*, 2nd Ed., Academic Press, 2003. 458
 17. D. K. Schroder, *Semiconductor Material and Device Characterization*, 3rd Ed.,
 459 Wiley-IEEE Press, 2006. 460
 18. T. Paloposki and L. Liedquist, *Steel emissivity at high temperatures*, VTT Tiedoteita
 461 - Research Notes 2299, pp. 81, 2005. 462
 19. C. E. Kennedy, *Review of Mid- to High- Temperature Solar Selective Absorber Ma-*
 463 *terials*, National Renewable Energy Laboratory (NREL), 2002. 464
 20. G. del Coso, C. Cañizo, and A. Luque, "Radiative energy loss in a polysilicon CVD
 465 reactor," *Solar Energy Materials & Solar Cells*, **95**, 1042 (2011). 466
 21. A. Ramos, C. del Cañizo, J. Valdehita, J. C. Zamorano, and A. Luque, "Radiation heat
 467 savings in polysilicon production: Validation of results through a CVD laboratory
 468 prototype," *Journal of Crystal Growth*, **374**, 5 (2013). 469
 22. R. Siegel and J. R. Howell, *Thermal radiation heat transfer*, McGraw-Hill, Siegel72,
 470 1972. 471
 23. G. del Coso, "Chemical decomposition of silanes for the production of solar grade
 472 silicon," Ph.D. Thesis, Universidad Politécnica de Madrid - ETSI Telecomunicación,
 473 2010. 474
 24. A. Ramos, C. del Cañizo, J. Valdehita, J. C. Zamorano, A. Rodríguez, and A. Luque,
 475 "Exploring polysilicon deposition conditions through a laboratory CVD prototype,"
 476 *Physica Status Solidi C*, **10** (2012) 477
 25. D. R. Lide (Ed.), *CRC Handbook of Chemistry and Physics*, National Institute of
 478 Standards and Technology, 2005. 479
 26. G. G. Gubareff, J. E. Janssen, and R. H. Torborg, *Thermal Radiation Properties*
 480 *Survey*, Honeywell Research Center, 1960. 481
 27. S. Grove, *Physics and Technology of Semiconductor Devices*, Willey, 1967. 482
 28. S. M. Sze, *Semiconductor Devices: Physics and Technology*, 2nd Ed., Willey, 2001. 483